Published in final edited form as:
J Neurochem. 2005 June ; 93(6): 1444–1453.

Myt1 family recruits histone deacetylase to regulate neural transcription

Elena Romm, **Joseph A. Nielsen**, **Jin G. Kim**, and **Lynn D. Hudson**

Section of Developmental Genetics, National Institute of Neurologic Disorders and Stroke, National Institutes of Health, Bethesda, Maryland, USA

Abstract

The myelin transcription factor 1 (*Myt1*) gene family is comprised of three zinc finger genes [*Myt1*, *Myt1L* (Myt1-Like) and NZF3] of the structurally unique CCHHC class that are expressed predominantly in the developing CNS. To understand the mechanism by which this family regulates neural differentiation, we searched for interaction partners. In both yeast and a mammalian two-hybrid system, Myt1 and Myt1L interacted with Sin3B, a protein that mediates transcriptional repression by binding to histone deacetylases (HDACs). Myt1–Sin3B complexes were co-immunoprecipitated from transfected mammalian cells and included HDAC1 and HDAC2. Myt1 and Myt1L could partner with all three Sin3B isoforms, the long form ($Sin3B_{LF}$) that includes the HDAC-binding domain, and the two short forms ($Sin3B_{SF293}$ and $Sin3B_{SF302}$) that lack this domain and may consequently antagonize $Sin3B_{LF}$/HDAC-mediated co-repression. Myt1 or Myt1L interactions with the HDAC-binding form of Sin3B conferred repression on a heterologous promoter. Oligodendrocytes were shown to express transcripts encoding each of the Sin3B isoforms. We present a model in which the Myt1 family of zinc finger proteins, when bound to a neural promoter, can recruit Sin3B. Depending on the relative availability of Sin3B isoforms, the *Myt1* gene family may favor the silencing of genes during neural development.

Keywords

histone deacetylase; mSin3; Myt1; repression; transcription; zinc finger

Abbreviations used

CMV, cytomegalovirus; GAPDH, glyceraldehyde-3-phosphate dehydrogenase; HDAC, histone deacetylase; Myt1, myelin transcription factor 1; Myt1L, myelin transcription factor 1 like; NZF, neural zinc finger; PAH, paired amphipathic helical

---

The specification and differentiation of neural cells is orchestrated at the transcriptional level by two classes of factors, those with chromatin-remodeling activities that regulate how tightly histones wrap up DNA in nucleosomal structures, and those that directly contact target genes and/or other transcription factors and ultimately determine whether the basal machinery initiates transcription. These two classes are functionally and physically linked, as co-activator complexes have an associated histone acetylase whose activity relaxes chromatin structure to promote accessibility of DNA-binding proteins, and co-repressor complexes have an opposing histone deacetylase (HDAC) activity (Wolffe *et al*. 2000). Key to this linkage are sequence-specific transcription factors that can recruit HDACs or acetylases. The zinc finger protein

Address correspondence and reprint requests to Lynn D. Hudson, Building 49, Room 5A82, 49 Convent Drive, Bethesda, MD 20892–4479, USA. E-mail: hudsonl1@od.nih.gov.

RE1-silencing transcription factor is one such factor that represses many neuron-specific genes through multiple HDAC complexes (Grimes *et al*. 2000; Ballas *et al*. 2001).

The myelin transcription factor 1 (Myt1) family represents neural zinc finger proteins of a structurally novel CCHHC class that were originally cloned by their binding to the promoter of the most abundantly expressed myelin gene, proteolipid protein (Kim and Hudson 1992). The consensus DNA-binding domain of the Myt1 family is Cys-X_4-Cys-X_4-His-X_7-His-X_5-Cys (also termed CCHHC domains). A novel fold arises from the coordination of a zinc ion to the three Cys residues and the second His residues, whereas the other conserved His residue is stacked between the zinc-coordinated His and an aromatic residue (Berkovits-Cymet *et al*. 2004).

Myt1 modulates the proliferation and differentiation of oligodendrocytes, the myelin-forming cell of the CNS (Nielsen *et al*. 2004). Moreover, overexpressed Myt1 promotes commitment to a neuronal fate in *Xenopus* (Bellefroid *et al*. 1996). Two additional Myt1 family members with selective neural expression were subsequently identified: Myt1-Like (Myt1L/neural zinc finger(NZF)-1/Png-1) and NZF-3/rMyT3 (Bellefroid *et al*. 1996; Jiang *et al*. 1996; Kim *et al*. 1997; Weiner and Chun 1997; Yee and Yu 1998). Both activator and repressor activities have been reported for the Myt1 family in transient transfection assays (Bellefroid *et al*. 1996; Jiang *et al*. 1996; Yee and Yu 1998). To define how the Myt1 family contributes to neural differentiation, we examined the interactions of Myt1 with other nuclear partners. Both Myt1 and Myt1L interacted with the co-repressor Sin3B, and the Myt1 complexes were shown to include HDAC1 and HDAC2. The Myt1 family exemplifies a class of neural sequence-specific transcription factors that actively recruit HDACs to selected genes during CNS development.

Experimental procedures

Screening for interaction partners in yeast

The following ‘bait’ plasmids were constructed using the primers listed below to subclone PCR-amplified portions of the *MYT1* (human) and *Myt1L* genes into the *Nde*I and *Bam*HI sites of the pAS2-1 binding domain (BD) vector (BD Biosciences Clontech, Palo Alto, CA, USA). pMYT1-CD contains the central domain (CD) of the human MYT1 cDNA between the cluster of two zinc fingers and the cluster of four zinc fingers (positions 502–1062 of the human sequence (Kim and Hudson 1992). pMyt1L-CD contains the central domain of the mouse Myt1L cDNA between the third and fourth fingers (positions 2560–3350 of the mouse sequence; Kim *et al*. 1997). Primers used for pMYT1-CD were 5′-GAA-TTCCATATGGATGCTCAGGTTTTTGGCAAAC-3′(forward) and 5′-GAATTCGGATCCCTGGCTCTGACTCCTCAGGTTC-3′(reverse); those for pMyt1L-CD were 5′-ACACACATATGCAGC-TTGAGATTCCTCAG-3′(forward) and 5′-CAACCGGATCCTTT-GCTTTCCTTGCACTG-3′(reverse).

Screening of a mouse brain cDNA library (pool of BALB/c males, 9–12 weeks of age) fused to the GAL4 activation domain in the pACT2 vector was carried out according to the manufacturer’s instructions (Clontech) using yeast strain CG-1945 and herring sperm DNA (Sigma, St Louis, MO, USA) as the carrier DNA. Following transformation, competent cells were spread on plates containing 5 mM 3-amino-1,2,4-triazole (a competitive inhibitor of the His3 protein) and lacking tryptophan, leucine and histidine. Colonies were transferred to Whatman no. 5 filters presoaked in X-gal substrate for staining of β-galactosidase.

Detecting interactions in a mammalian two-hybrid system

Mouse Myt1 and Myt1L were tested for interactions with Sin3B using the yeast GAL4 DNA-binding domain in the pBIND vector (Promega, Madison, WI, USA) for the Myt1/Myt1L constructs and the herpes simplex virus VP16 activation domain (AD) in pACT (Promega) for the Sin3B constructs. The regions used included the entire central domain of Myt1 (bases 2035–2739; amino acids 502–736), the first half of the Myt1 central domain (bases 2035–2399; amino acids 502–623), the second half of the Myt1 central domain (bases 2380–2739; amino acids 617–736), and the Myt1L central domain (bases 2655–3416; amino acids 642–896). A truncated form of Sin3B called $Sin3B_{SF274}$ (bases 13–834, corresponding to the amino terminal 274 amino acids of Sin3B; David *et al*. 1998) was identified as an interacting partner of Myt1 in the yeast two-hybrid screen. $Sin3B_{SF274}$ was amplified with the proofreading polymerase PfuTurbo (Stratagene, La Jolla, CA, USA) for three cycles of denaturation at 94°C for 1 min, annealing at 45°C for 2 min and extension at 68°C for 3 min, followed by 25 cycles of 94°C for 1 min, annealing at 55°C for 2 min and extension at 68°C for 3 min. Gel-purified PCR products were directionally subcloned into pBIND (Myt1) or pACT (Sin3B) and sequenced.

The following primers were used to make the different Myt1 and Sin3B domains: $Myt1_{2035–2739}$ and $Myt1_{2035–2399}$, 5′-CCAAGGAT-CCTTAAGCAGCTTGAGGTTCCACC-3′ (forward); $Myt1_{2035–2739}$ and $Myt1_{2380–2739}$, 5′-CTTTGCGGCCGCAAAGTTGGTTAGGGTG-ACTT-3′ (reverse); $Myt1_{2035–2399}$, 5′-AATTGCGGCCGCAAGTCCA-GAGTTCCATTCTC-3′ (reverse); $Myt1_{2380–2739}$, 5′ CCAAGGATC-CGCGAGAATGGAACTCTGGACTT-3′ (forward); $Myt1L_{2655–3416}$, 5′-GCGCGGATCCGGTTTGAGTACAACAGTTACG-3′ (forward) and 5′-CCGGAATCTAGAACTGGTGGCCAGCATACTTC-3′ (reverse); $Sin3BSF274_{13–834}$, 5′-AATTGGATCCAAATGGCGCATGC-AGGCAGCGG-3′ (forward) and 5′-GAATATGGTACCCTTGGCT-GGCGCAGACACAG-3′ (reverse); Sin3BPAH2, 5′-AAGGAT-CCAGGTGCCCCTGGAGTCTG-3′ (forward) and 5′-GAGGT-ACCTCAGGCAGGAACTGTCCGA-3′ (reverse).

In the mammalian two-hybrid assay, COS-1 cells (ATCC, Manassas, VA, USA) or CG4 cells (Louis *et al*. 1992) were transfected with Lipofectamine 2000 (Invitrogen, Carlsbad, CA, USA) for 6 h in OPTI-MEM (Invitrogen), then switched to Dulbecco's modified Eagle's medium with 10% fetal calf serum and harvested at 24–48 h. Renilla and firefly luciferase were quantitated using the Promega Dual-Luciferase reporter assay system. Positive controls included the combination of the pBIND-Id and pACT-MyoD plasmids.

For testing interactions between Myt1/Myt1L and Sin3B on a heterologous promoter, fusions between the GAL4 DNA-binding domain and the central domain of Myt1 or Myt1L (pBIND-$Myt1_{502–736}$, pBIND-$Myt1_{502–623}$, pBIND-Myt1617–736 and pBIND-$Myt1L_{642–896}$) were co-transfected into COS-1 cells with the pG5 promoter reporter plasmid containing five copies of the GAL4-binding site as well as a minimal promoter driving expression of firefly luciferase (Promega) together with various Sin3B isoforms shown in Fig. 1(a) (pcDNA-$Sin3B_{SF293}$, pcDNA-$Sin3B_{SF302}$ and $Sin3B_{LF}$).

Co-immunoprecipitation of Myt1/Myt1L with Sin3B and HDACs

The nuclear proteins were prepared from COS-1 cells co-transfected using Lipofectamine 2000 with a combination of $Sin3B_{SF274}$ and $Myt1_{502–736}$ and immunoprecipitated as detailed previously (Grimes *et al*. 2000). In the experiments done in HEK 293 cells, the immunoprecipitation buffer and washing buffer were modified by addition of $ZnCl_2$ (0.2 mM), 1% Triton X-100 and 0.5% (octylphenoxy)polyethoxyethanol. The concentration of $NaCl_2$ was also increased from 150 m_M to 250 m_M in the wash buffer. For experiments requiring the full-length Myt1, a plasmid in which expression of the seven zinc finger isoform of Myt1 that

was Myc-epitope tagged (Myt1Myc) and driven by the cytomegalavirus (CMV) promoter was used (Nielsen *et al*. 2004). For experiments requiring the long form of Sin3B, a flag epitope-tagged version called $Sin3B_{LF}$ (a gift from R. DePinho and A. Dejean, Harvard Medical School), in which the CMV promoter drives the expression of $Sin3B_{LF}$, was used. The two short forms of Sin3B ($Sin3B_{SF293}$ and $Sin3B_{SF302}$) were subcloned into the pcDNA3.Myc vector using the following primers: $Sin3B_{SF293}$ and $Sin3B_{SF302}$, 5′-AAG-GATCCAACATGGCGCATGCAGGC-3′ (forward); $Sin3B_{SF293}$, 5 ′-AAGGTACCACTCCTCAGCTGTGCAGTAACC-3′ (reverse); and $Sin3B_{SF302}$, 5′-ATGGTACCTGGCTCTGGCCTCAGGCTCC-3′ (reverse).

Antibodies for precipitation or immunoblot detection included: rabbit anti-mSin3B (A-20; Santa Cruz Biotechnology, Santa Cruz, CA, USA) or rabbit anti-mSin3B (AK-12; Santa Cruz Biotechnology) biotinylated according to the manufacturer's instructions (Pierce, Rockford, IL, USA) for use as a detecting antibody, rabbit anti-Myt1-His and anti-Myt1-D (Armstrong *et al*. 1995), mouse anti-GAL4DNA-BD monoclonal antibody (Clontech), rabbit anti-GAL4 (USBiological, Swampscott, MA, USA), mouse anti-c-Myc (Sigma), mouse anti-HDAC1 (Santa Cruz Biotechnology), rabbit anti-HDAC1 (ABR, Golden, CO, USA), and goat anti-HDAC1, rabbit anti-HDAC2, mouse anti-HDAC2, rabbit anti-HDAC3, rabbit anti-HDAC4, goat anti-HDAC4, rabbit anti-HDAC7, goat anti-HDAC7, rabbit anti-HDAC8 and mouse anti-HDAC8 (all from Santa Cruz Biotechnology). Immunoprecipitated proteins were electrophoresed on Bis–Tris gels with SeeBlue Plus2 prestained molecular weight markers (Invitrogen, Carlsbad, CA, USA), transferred to membranes and stained with Ponceau S (Sigma). Peroxidase-conjugated secondary antibodies, including goat anti-mouse IgG, goat anti-rabbit IgG and rabbit anti-goat IgG (all from Pierce), and NeutrAvidin (Pierce) were visualized with an ECL kit (Amersham-Pharmacia, Piscataway, NJ, USA).

Semiquantitative RT–PCR of Sin3B isoforms

Whole brains were dissected from P7 mice, and the cerebellum and meninges were removed. The brains were triturated, digested with papain and Dnase, layered on to a 15–40% Percoll gradient and centrifuged at 2000 *g* for 15 min at 4°C. Oligodendrocyte progenitors were identified using the A2B5 mouse monoclonal IgM antibody (Eisenbarth *et al*. 1979) conjugated with biotin for detection with streptavidin conjugated with phycoerythrin and texas red. More mature oligodendrocyte lineage cells were identified with O4 mouse monoclonal IgM (Sommer and Schachner 1981) directly conjugated with Alexa Fluor 488. Labeled cell suspensions were sorted using a FACSVantageSE flow cytometer (Becton Dickinson, Mountain View, CA, USA). Oligodendrocyte progenitors were sorted as A2B5 + O4 –, and the more mature oligodendrocytes were sorted as A2B5 –, O4 + (Maric *et al*. 2003). FITC and phycoerythrin–texas red were excited by an argon laser tuned to 488 nm (Enterprise II, Coherent, Santa Clara, CA, USA) and the resulting emission was collected with 530 ± 30 nm and 615 ± 10 nm bandpass filters. The cells were sorted into appropriate tubes based on fluorescent signal intensity. RNA was extracted using RNeasy (Qiagen, Valencia, CA, USA). Reverse transcriptase reactions were set up with 0.2 μg total RNA and oligodT primers using the Superscript First-Strand Synthesis System (Invitrogen) according to the manufacturer's instructions. PCR amplification was carried out using a common Sin3B forward primer and unique Sin3B reverse primers to identify the different Sin3B isoforms: Sin3B, 5′-ACACC-TACCAGAAGGAACAGC-3′ (forward); $Sin3B_{LF}$, 5′-CCAGG-AATGGACTGACAAGC-3′ (reverse); $Sin3B_{SF302}$, 5′-GAGAAC-CCACACATGGAC-3′ (reverse); and $Sin3B_{SF293+302}$, 5′-CACAT-TTCAACTGCAGCC-3′ (reverse). Glyceraldehyde-3-phosphate dehydrogenase (GAPDH) primers used were 5′-GAGCTG-AACGGGAAGCTCAC-3′ (forward) and 5′-CACCACCCTG-TTGCTGTAGC-3′ (reverse).

The specificity of each primer pair was tested by amplifying $Sin3B_{LF}$, $Sin3B_{SF293}$ and $Sin3B_{SF302}$ plasmid templates with each primer pair and confirming primer pair amplification of the appropriate template (data not shown). Despite the high degree of sequence homology between the two short forms ($Sin3B_{SF293}$ and $Sin3B_{SF302}$), one primer combination was found that resulted in the selective amplification of $Sin3B_{SF302}$. The amplification was performed with a 2700 PCR machine (Applied Biosystems, Foster City, CA, USA) with a 2-min predenaturation at 95°C, denaturation for 30 s at 95°C, annealing for 30 s at 61°C, and extension for 1 min at 72°C. Semiquantitative RT–PCR was performed by starting with 35 PCR cycles and then reducing the number of PCR cycles by three until product could no longer be visualized on a 1% agarose gel. The number of cycles one step above the cycle number at which no product could be visualized on a 1% agarose gel was used to assess the amount of product formed during the linear range of the PCR amplification reaction. A control reaction lacking reverse transcriptase was used to confirm the absence of genomic DNA contamination.

Results

MYT1 and Myt1L interact with the transcriptional co-repressor Sin3B in yeast

To gain insight into the molecular mechanism by which MYT1 bound to DNA via its zinc fingers affects transcription, a screen for interacting proteins was carried out in a yeast system. For this screen, the portion of the MYT1 protein located between the two clusters of zinc fingers (termed the 'central domain') was fused to the GAL4 DNA-binding domain to serve as 'bait'. In a screen of over 1×10^6 colonies from a 9–12-week mouse brain cDNA library in which open reading frames were fused to the GAL4 activation domain of pACT2, 15 positive clones were partially sequenced. Clones encoding nuclear proteins were tested in subsequent screens in which yeast were consecutively transformed with the bait and prey plasmids. The two clones that survived this selection were sequenced in entirety and identified as corresponding to the first 274 amino acids of Sin3B (accession no. L38622). The murine *Sin3B* gene is alternatively spliced to generate the three isoforms previously described by Georgopoulos and co-workers as a 'long form' and 'short forms' (Koipally *et al*. 1999), each of which can be distinguished by a unique carboxy terminus: $Sin3B_{LF}$, $Sin3B_{SF293}$ and $Sin3B_{SF302}$ (Fig. 1a). The Sin3B clones isolated from the yeast screen correspond to the two 'short forms' of Sin3B ($Sin3B_{SF293}$ and $Sin3B_{SF302}$), both of which contain only the first two of the four paired amphipathic helical (PAH) domains present in the 'long form' ($Sin3B_{LF}$; Fig. 1a).

The central domain of MYT1 that interacts with Sin3B displays 54% amino acid identity with the corresponding region of Myt1L (Kim *et al*. 1997). To determine whether Myt1L is also a partner of Sin3B, yeast cells were simultaneously transformed with the $Sin3B_{274}$ activation domain plasmid and either the MYT1 or the Myt1L expression plasmids. Both MYT1 and Myt1L plasmids produced colonies with β-galactosidase activity in conjunction with Sin3B (Fig. 1c). Singly transformed colonies produced no activity; nor did a combination of the MYT1 plasmids with the 'empty' GAL4 activation domain vector, or the p53-binding domain control vector together with GAL4 activation domain (Fig. 1c). The blue β-galactosidase staining observed in the MYT1/Myt1L co-transformations with Sin3B was as robust as that seen with the strong interactors p53 and SV40T antigen (Fig. 1c).

Myt1 and Myt1L interact with the transcriptional co-repressor Sin3B in a mammalian two-hybrid system

To verify the interactions observed in the yeast two-hybrid system, as well as to further define the Myt1 and Sin3B domains that participate in this interaction, we used a mammalian system. Portions of the mouse *Myt1* gene (shown schematically in Fig. 1b), including the entire central domain ($Myt1_{502–736}$), the amino terminal half of the central domain ($Myt1_{502–623}$), the carboxy terminal half of the central domain ($Myt1_{617–736}$) and the mouse Myt1L central

domain ($Myt1L_{642–896}$) were tested for interaction with $Sin3B_{274}$ in COS-1 cells. When co-transfected with $Sin3B_{274}$, the central domains of Myt1 and Myt1L each produced a fourfold increase in reporter activity over controls (Fig. 1d). The amino terminal half of the central domain ($Myt1_{502–623}$) also displayed full activity, whereas the carboxy terminal half ($Myt1_{617–736}$) had no activity above background. These results localize the interaction domain to amino acids 502–623 of Myt1. This latter region is well conserved among the three branches of the Myt1 family (Myt1, Myt1L and NZF–3) and includes three predicted amphipathic α-helices (Fig. 2).

Sin3B binds a number of transcription factors through one or more PAH domains (Brubaker *et al*. 2000; Spronk *et al*. 2000). To delineate further the Myt1/Myt1L-interacting subdomain of Sin3B, which in the yeast two-hybrid system was identified as the first 274 amino acids shared by all Sin3B isoforms, the second PAH domain ($Sin3B_{PAH2}$) was compared with one of the Sin3B isoforms containing the first two PAH domains ($Sin3B_{274}$). When co-transfected with the central domain of Myt1 or Myt1L, enhanced luciferase activity was evident with either one PAH domain of Sin3B ($Sin3B_{PAH2}$) or two PAH domains of Sin3B ($Sin3B_{274}$) fused to the activation domain of VP16 (Fig. 3a). However, $Sin3B_{274}$ containing both PAH domains had considerably enhanced interaction with Myt1 and Myt1L: 10-fold increases in luciferase activity over control versus a 2-fold increase for a single PAH domain. The carboxy terminal half of Myt1 ($Myt1_{617–736}$) had no activity above background. These results suggest that the interaction subdomain within Sin3B extends beyond a single PAH domain and confirm that Myt1 can potentially interact with all three alternatively spliced Sin3B isoforms in COS-1 cells.

To confirm that these interactions occur in a more relevant cell type, the experiments were repeated in an oligodendrocyte cell line, CG4 cells (Louis *et al*. 1992). Very similar interactions were detected in CG4 cells, with an approximately 2-fold increase observed with $Myt1_{502–623}$ and $Sin3B_{274}$ and a 3.5-fold increase with Myt1L and $Sin3B_{274}$ (Fig. 3b). The Myt1–Sin3B interactions were present but less pronounced in CG4 cells, possibly owing to competition with the endogenous Myt1 found in CG4 cells. The carboxy terminal half ($Myt1_{617–736}$) of the central domain displayed no activity above background in CG4 cells, a pattern first observed in COS-1 cells.

Sin3B co-precipitates with Myt1 in mammalian cells

To demonstrate the physical association of Myt1 and Sin3B in mammalian cells, the interacting domains of these two proteins were expressed in COS-1 cells before immunoprecipitation. The central domain of Myt1 ($Myt1_{502–736}$) was cloned into the pBIND vector to produce a GAL4 fusion protein in which the GAL4 portion was 147 amino acids (18 kDa). The resultant 46-kDa GAL4-$Myt1_{502–736}$ fusion protein was expected to be both detected and immunoprecipitated with either Myt1 or GAL4 antibodies. A truncated short form of Sin3B, $Sin3B_{274}$ (274 amino acids, 33 kDa) was fused to the VP16 protein of the pACT vector (65 amino acids, 8 kDa) to produce a 41-kDa protein.

As shown in Fig. 4, Myt1–Sin3B complexes were immunoprecipitated with either mSin3B antibodies (Figs 4a–c, lanes 1–5) or Myt1 antibodies (Figs 4a–c, lanes 6–10). The partners of the precipitated complexes were detectable using antibodies directed against either GAL4 (Fig. 4a), Myt1 (Fig. 4b), or mSin3B (Fig. 4c). No complexes were detected in COS-1 cells that were not transfected (lanes 1 and 6), as expected because of the absence of endogenous Myt1 mRNA in COS-1 cells (data not shown); nor were complexes detected when only the pACT (lane 2) or the pBIND (lane 7) vector was transfected into COS-1 cells. A small amount of complexes was present in cells that were transfected with the Myt1 plasmid only (Figs 4a and b, lane 4), indicating that the endogenous Sin3B was available for association with Myt1. The amount of complex formation greatly increased when the Myt1 and Sin3B plasmids were co-transfected (Figs 4a and b, lane 5).

These co-immunoprecipitation results validate the interactions detected between individual domains of Sin3B and Myt1/Myt1L in the two hybrid systems. To extend the results to native, full-length proteins, the co-immunoprecipitation experiments were repeated using plasmids encoding a Myc-epitope-tagged Myt1 (Myt1Myc; Nielsen *et al*. 2004) together with the long form of Sin3B ($Sin3B_{LF}$). Following precipitation with an antibody directed against Sin3B, full-length Myt1 could be detected in cells transfected with Myt1 alone (Fig. 5a, lane 7), which was presumably mediated by endogenous Sin3B. Myt1 was immunoprecipitated to a greater extent in cells co-transfected with both the Sin3B and Myt1 plasmids (Fig. 5a, lane 8).

Myt1 complexes contain HDACs 1 and 2

To identify which HDACs participate in Myt1 complexes, cells transfected with the Myc-epitope-tagged Myt1 (Myt1-Myc) and the long form of Sin3B ($Sin3B_{LF}$) were subjected to immunoprecipitation using antibodies directed against HDAC1, HDAC2, HDAC3, HDAC4, HDAC7 and HDAC8 (Figs 5b and c). The HDAC1 antibody precipitated Myt1 (Fig. 5b, lanes 3 and 4) when only endogenous Sin3B was available (lane 3) and to a greater extent in the presence of co-transfected $Sin3B_{LF}$ (Fig. 5b, lane 4). The HDAC2 antibody precipitated Myt1 to a lesser degree from cells co-transfected with Myt1Myc and $Sin3B_{LF}$ (Fig. 5b, lane 5). HDAC1 was also able to precipitate $Sin3B_{LF}$ (Fig. 5d, lane 6). Conversely, immunoprecipitations were also performed with Sin3B as a precipitating antibody and detection with an antibody to HDAC2. In these experiments, when $Sin3B_{LF}$ was transfected the approximately 60-kDa HDAC2 was detected (Fig. 5d, lane 3). There was no HDAC2 detection with the short form of $Sin3B_{274}$ or $Sin3B_{PAH}$, which both lack the HDAC domain (Figs 5, lanes 1 and 2), indicating the requirement of the HDAC binding domain for mSin3B–HDAC interaction (Alland *et al*. 1997).

Sin3B interactions with Myt1 or Myt1L confer repression on a heterologous promoter

To determine whether the interactions between Myt1 and Sin3B affect promoter activity, the three different Sin3B isoforms ($Sin3B_{SF293}$, $Sin3B_{SF302}$ and $Sin3B_{LF}$) were co-transfected with portions of Myt1 or MytlL fused to the GAL4 DNA-binding domain and the activity of the pG5 promoter (which contains five GAL4-binding sites) was assessed by measuring luciferase reporter levels (Fig. 6). All Sin3B isoforms reduced luciferase reporter activity when combined with Myt1 or Myt1L. The combination of the central domain of Myt1L and $Sin3B_{SF302}$ produced a 4-fold reduction in reporter activity. As an additional control, the carboxy terminal portion of the Myt1 central domain ($Myt1_{617–736}$), which did not interact with Sin3B in the assay shown in Fig. 3, did not affect pG5 promoter activity when co-transfected with any of the Sin3B isoforms.

Oligodendrocyte progenitors express both short and long forms of Sin3B

The expression of Sin3B isoforms during oligodendrocyte development was assessed by semiquantitative RT–PCR of oligodendrocyte populations purified using flow cytometry. Oligodendrocyte progenitors were sorted by their surface expression of the A2B5 glycolipid, and a more mature oligodendrocyte population was purified using antibodies directed against another surface lipid, O4. Three different primer pairs were designed to distinguish the $Sin3B_{LF}$, $Sin3B_{SF293}$ and $Sin3B_{SF302}$ isoforms. Oligodendrocytes expressed all three isoforms of Sin3B at both the oligodendrocyte progenitor stage and the more mature O4-positive stage (Fig. 7). At both developmental stages, the combined level of Sin3B short forms ($Sin3B_{SF293}$ and $Sin3B_{SF302}$) predominated (Fig. 7b).

Discussion

Defining the mode of action for a transcription factor involves identifying its interaction partners, both the factors contacted within a transcription complex and the target genes bound

through sequence-specific interactions. Here we provide the first evidence that the Myt1 family of CCHHC zinc finger proteins can recruit the co-repressor Sin3B. Myt1 and Myt1L interact with Sin3B in yeast and mammalian two-hybrid systems (Fig. 1), and these interactions confer repression on a heterologous promoter (Fig. 6). Complexes of Myt1 and Sin3B include two class I HDACs, HDAC1 and HDAC2 (Fig. 5). Sin3B modifies chromatin structure by binding class I HDACs (Wolffe *et al*. 2000). In addition to the HDAC-binding domain, the Sin3B protein contains four PAHs that can associate with an array of DNA-binding transcription factors. The helices of PAH2 form a hydrophobic cleft surrounding an amphipathic α-helix of the Mad repressor (Brubaker *et al*. 2000;Spronk *et al*. 2000), and the amphipathic α-helices present in the Sin3B-interacting central domain of the Myt1 family (Fig. 2) are similarly likely to be involved in a 'wedged helical bundle' with PAH1 or PAH2. The domain of the mammalian Myt1 that interacts with Sin3B corresponds to the portion of the *Xenopus* Myt1 protein essential for promoting commitment to a neuronal fate (Bellefroid *et al*. 1996). The homologous central domain region of Myt1L, located between the clusters of zinc finger DNA-binding domains, similarly interacts with the PAH1 and PAH2 domains of Sin3B (Fig. 3). Althought Sin3B typically behaves as a 'silencer' via recruitment of HDAC, the *Sin3B* gene can be alternatively spliced to generate the full-length protein as well as two short forms ($Sin3B_{SF293}$ and $Sin3B_{SF302}$) lacking the HDAC-binding domain defined by DePinho and co-workers (Alland *et al.* 1997). Contradictory results regarding whether the short forms of Sin3B bind directly to HDACs (Alland *et al.* 1997;Koipally *et al.* 1999) may be explained by the ability of all Sin3B isoforms to interact with the co-repressor N-CoR protein (Alland *et al*. 1997) and thereby participate in additional multiprotein complexes that mediate transcriptional repression (Jepsen and Rosenfeld 2002;de Ruijter *et al*. 2003).

The potential for different regulatory outcomes with different Sin3B isoforms prompted us to explore whether cells of the oligodendrocyte lineage possess all three isoforms of Sin3B. At both the progenitor stage and a more mature stage of oligodendrogenesis, cells were shown to express the long form of Sin3B as well as the short forms ($Sin3B_{SF293}$ and $Sin3B_{SF302}$). Thus, Myt1 may participate in a number of complexes in a promoter-specific fashion, and the predominance of complexes containing short forms of Sin3B may serve to reduce the HDAC1 and HDAC2-related repressor activity of these complexes.

Myt1 figures in neural cell differentiation, both in the specification of neurons (Bellefroid *et al*. 1996) and in the proliferation and differentiation of oligodendrocytes (Nielsen *et al*. 2004). In *Xenopus*, Myt1 acts synergistically with neurogenin (NGN1) in the Notch signaling pathway (Bellefroid *et al*. 1996; Quan *et al*. 2004) to promote neuronal differentiation. Myt1 may also be necessary for endocrine islet development, in which it participates in the same pathway as NGN3 (Gu *et al*. 2004). We present a model in which the Myt1/Myt1L/NZF-3 family of zinc finger proteins links transcriptional activity and local chromatin structure in the developing mammalian nervous system. Although all three family members are expressed early, only Myt1 is expressed in developing oligodendrocytes (Armstrong *et al*. 1995). Myt1 is also found in neural precursors and in some subpopulations of mature neurons (Bellefroid *et al*. 1996; Kim *et al*. 1997). Myt1L appears restricted to recently born, post-mitotic neurons in the CNS (Kim *et al*. 1997; Weiner and Chun 1997), but is also detected in the pituitary (Jiang *et al*. 1996). The set of target genes contacted by each family member is likely to be distinct, although in each case Myt1/Myt1L binding can recruit HDACs to those promoters, with an accompanying localized hypo-acetylation of core histones and resultant transcriptional repression. Another scenario is anticipated in the face of sufficient $Sin3B_{SF}$ (lacking the HDAC domain): $Sin3B_{SF}$–Myt1 complexes bound to target genes may preclude or modulate deacetylase binding, leading to a state of transcriptional activation. Unraveling the balance between these transcriptional states will require an investigation of the developmental regulation of Myt1 complex formation in different neural populations.

Acknowledgements

The authors thank Drs R. DePinho and A. Dejean for the gift of plasmids and Dr Heinz Arnheiter for helpful discussions. The cloning efforts of Dr Nam Woo Kim in the initial stages of this study and the sequencing carried out by James Nagle (National Institute of Neurologic Disorders and Stroke (NINDS) Sequencing Facility) are much appreciated. We thank Dr Dragan Maric (Laboratory of Neurophysiology, NINDS) for the flow cytometry used to isolate pure oligodendrocytes and Jodi Berndt for the culturing of CG4 cells. Support was from intramural NINDS funds.

References

Alland L., Muhle R.; Hou H. Jr, Potes J.; Chin L., Schreiber-Agus N.; DePinho, RA. Role for N-CoR and histone deacetylase in Sin3-mediated transcriptional repression. Nature 1997;387:49–55. [PubMed: 9139821]

Armstrong R. C., Kim J. G; Hudson, LD. Expression of myelin transcription factor I (MyTI), a 'zinc-finger' DNA-binding protein, in developing oligodendrocytes. Glia 1995;14:303–321. [PubMed: 8530187]

Ballas N, Battaglioli E, Atouf F, et al. Regulation of neuronal traits by a novel transcriptional complex. Neuron 2001;31:353–365. [PubMed: 11516394]

Bellefroid E. J., Bourguignon C.; Hollemann T., Ma Q.; Anderson D. J., Kintner C.; Pieler, T. X-MyT1, a *Xenopus* C2HC-type zinc finger protein with a regulatory function in neuronal differentiation. Cell 1996;87:1191–1202. [PubMed: 8980226]

Berkovits-Cymet H. J., Amann B. T; Berg, JM. Solution structure of a CCHHC domain of neural zinc finger factor-1 and its implications for DNA binding. Biochemistry 2004;43:898–903. [PubMed: 14744132]

Brubaker K., Cowley S. M; Huang K., Loo L.; Yochum G. S., Ayer D. E; Eisenman, RN.; Radhakrishnan, I. Solution structure of the interacting domains of the Mad–Sin3 complex: implications for recruitment of a chromatin-modifying complex. Cell 2000;103:655–665. [PubMed: 11106735]

David G., Alland L.; Hong S. H., Wong C. W; DePinho, RA.; Dejean, A. Histone deacetylase associated with mSin3A mediates repression by the acute promyelocytic leukemia-associated PLZF protein. Oncogene 1998;16:2549–2556. [PubMed: 9627120]

Eisenbarth G. S., Walsh F. S; Nirenberg, M. Monoclonal antibody to a plasma membrane antigen of neurons. Proc Natl Acad Sci USA 1979;76:4913–4917. [PubMed: 388422]

Grimes J. A., Nielsen S. J; Battaglioli E., Miska E. A; Speh J. C., Berry D. L; Atouf F., Holdener B. C; Mandel, G.; Kouzarides, T. The co-repressor mSin3A is a functional component of the REST–CoREST repressor complex. J Biol Chem 2000;275:9461–9467. [PubMed: 10734093]

Gu G., Wells J. M; Dombkowski D., Preffer F.; Aronow, B.; Melton, DA. Global expression analysis of gene regulatory pathways during endocrine pancreatic development. Development 2004;131:165–179. [PubMed: 14660441]

Jepsen K, Rosenfeld MG. Biological roles and mechanistic actions of co-repressor complexes. J Cell Sci 2002;115:689–698. [PubMed: 11865025]

Jiang Y.Yu V. C., Buchholz F.; O'Connell S., Rhodes S. J; Candeloro C., Xia Y. R; Lusis, AJ.; Rosenfeld, MG. A novel family of Cys-Cys, His-Cys zinc finger transcription factors expressed in developing nervous system and pituitary gland. J Biol Chem 1996;271:10723–10730. [PubMed: 8631881]

Kim JG, Hudson LD. Novel member of the zinc finger superfamily: a C2-HC finger that recognizes a glia-specific gene. Mol Cell Biol 1992;12:5632–5639. [PubMed: 1280325]

Kim J. G., Armstrong R. C. V; Agoston D., Robinsky A.; Wiese C., Nagle J.; Hudson, LD. Myelin transcription factor 1 (Myt1) of the oligodendrocyte lineage, along with a closely related CCHC zinc finger, is expressed in developing neurons in the mammalian central nervous system. J Neurosci Res 1997;50:272–290. [PubMed: 9373037]

Koipally J., Renold A.; Kim, J.; Georgopoulos, K. Repression by Ikaros and Aiolos is mediated through histone deacetylase complexes. EMBO J 1999;18:3090–3100. [PubMed: 10357820]

Louis J. C., Muir D.; Varon, S. Autocrine inhibition of mitotic activity in cultured oligodendrocyte-type-2 astrocyte (O-2A) precursor cells. Glia 1992;6:30–38. [PubMed: 1387386]

Maric D., Maric I.; Chang, YH.; Barker, JL. Prospective cell sorting of embryonic rat neural stem cells and neuronal and glial progenitors reveals selective effects of basic fibroblast growth factor and

epidermal growth factor on self-renewal and differentiation. J Neurosci 2003;23:240–251. [PubMed: 12514221]

Nielsen J. A., Berndt J. A; Hudson, LD.; Armstrong, RC. Myelin transcription factor 1 (Myt1) modulates the proliferation and differentiation of oligodendrocyte lineage cells. Mol Cell Neurosci 2004;25:111–123. [PubMed: 14962745]

Quan X. J., Denayer T.; Yan J., Jafar-Nejad H.; Philippi A., Lichtarge O.; Vleminckx, K.; Hassan, BA. Evolution of neural precursor selection: functional divergence of proneural proteins. Development 2004;131:1679–1689. [PubMed: 15084454]

de Ruijter A. J., van Gennip A. H; Caron H. N., Kemp S.; van, Kuilenburg A. B. Histone deacetylases (HDACs): characterization of the classical HDAC family. Biochem J 2003;370:737–749. [PubMed: 12429021]

Sommer I, Schachner M. Monoclonal antibodies (O1 to O4) to oligodendrocyte cell surfaces: an immunocytological study in the central nervous system. Dev Biol 1981;83:311–327. [PubMed: 6786942]

Spronk C. A., Tessari M.; Kaan A. M., Jansen J. F; Vermeulen M., Stunnenberg H. G; Vuister, GW. The Mad1–Sin3B interaction involves a novel helical fold. Nat Struct Biol 2000;7:1100–1104. [PubMed: 11101889]

Weiner JA, Chun J. Png-1, a nervous system-specific zinc finger gene, identifies regions containing postmitotic neurons during mammalian embryonic development. J Comp Neurol 1997;381:130–142. [PubMed: 9130664]

Wolffe A. P., Urnov F. D; Guschin, D. Co-repressor complexes and remodelling chromatin for repression. Biochem Soc Trans 2000;28:379–386. [PubMed: 10961924]

Yee KS, Yu VC. Isolation and characterization of a novel member of the neural zinc finger factor/myelin transcription factor family with transcriptional repression activity. J Biol Chem 1998;273:5366–5374. [PubMed: 9478997]

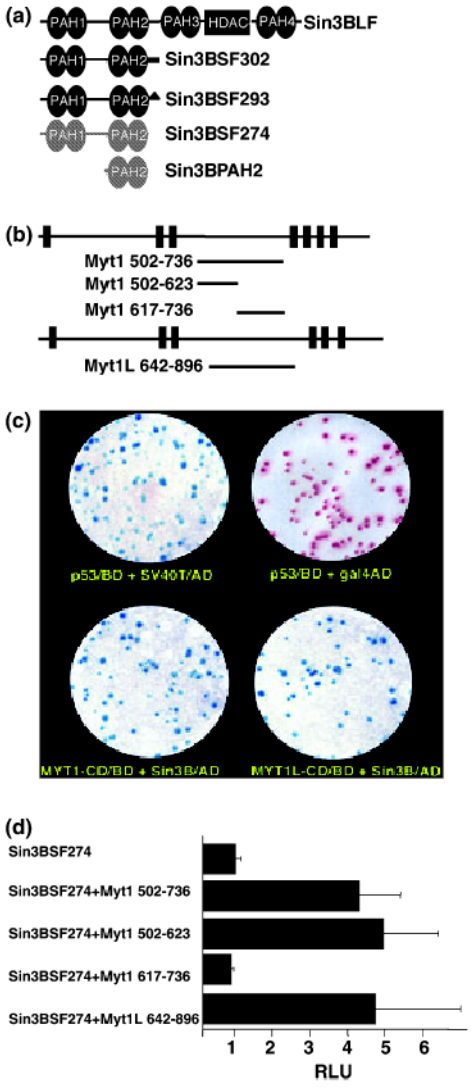

Fig. 1.

Sin3B is an interacting partner for MYT1 and MYT1L in a yeast and a mammalian two-hybrid system. (a) The mouse 955- amino acid Sin3B long form ($Sin3B_{LF}$) and the alternatively spliced short forms ($Sin3B_{SF293}$ and $Sin3B_{SF302}$) are schematized, with the four PAHs represented by intersecting ovals and the HDAC binding domain boxed. The portion of Sin3B (the first 274 amino acids) present as the GAL4 activation domain fusion protein used in the yeast system (c) is shown as $Sin3B_{SF274}$, and the single PAH helix used in Fig. 3 is shown as $Sin3B_{PAH2}$. (b) Constructs depicted in the schematic include the entire central domain of Myt1 from amino acids 502–736 ($Myt1_{502–736}$), the amino half of the Myt1 central domain ($Myt1_{502–623}$), the carboxy half of the Myt1 central domain ($Myt1_{617–736}$) and the entire central domain of Myt1L ($Myt1L_{642–896}$). The zinc finger DNA-binding domains of Myt1 and Myt1L are represented by black boxes. (c) β-Galactosidase-stained filters from CG-1945 cells co-transformed with either control plasmids p53 protein fused to the GAL4-binding domain (p53/BD) with the SV40T antigen fused to the GAL4 activation domain (SV40T/AD) (top left) or with the vector alone (GAL4AD) (top right). Bottom panels show filters for the mouse $Sin3B_{SF274}$ domain extending from amino acids 1–274 fused to the GAL4 activation domain ($Sin3B_{274}$/AD) with the central domain of the human MYT1 (bottom left) or the murine Myt1L

(bottom right) fused to the GAL4-binding domain (MYT1-CD/BD and Myt1L-CD/BD respectively). (d) Interaction of the central domains of murine Myt1 and Myt1L with $Sin3B_{SF274}$ in COS-1 cells. COS-1 cells were assayed for firefly and renilla luciferase activity 24–48 h after transfection with mouse $Sin3B_{SF274}$ and one of the mouse MYT1/MYT1L plasmids. Results are expressed as the ratio of firefly to renilla luciferase light units (RLU), normalized to the appropriate control transfection in which only the pBIND vector (lacking Sin3B) was co-transfected with the Myt1 expression plasmid. Values are mean ± SD of six independent measurements.

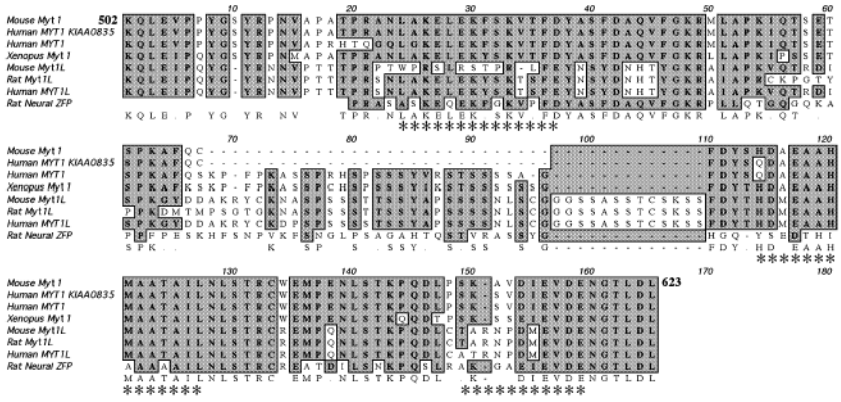

Fig. 2.

Sequence similarities in the Sin3B-binding domain of Myt1 family members. Members aligned by MacVector 7.0 for the 122 amino acid mSin3B interaction domain of the mouse Myt1 ($Myt1_{502–623}$) are: Myt1 [mouse AF004294 (Kim et al. 1997); human KIAA0835, gi11323191 and M96980 (Kim and Hudson 1992); Xenopus U67078 (Bellefroid et al. 1996)], Myt1L [mouse AF004295 (Kim et al. 1997); rat NZF-1, U48809 (Jiang et al. 1996); human AF036943] and NZF-3/MyT3 (neural ZFP) [AF031942 (Yee and Yu 1998) and U67080]. Identical amino acid residues are shown in boldface and boxed in gray. The Chou–Fasman α-helices (indicated by asterisks) were found to have amphipathic character using the HelicalWheel plot of the GCG program, National Institutes of Health, Bethesda, MD, USA.

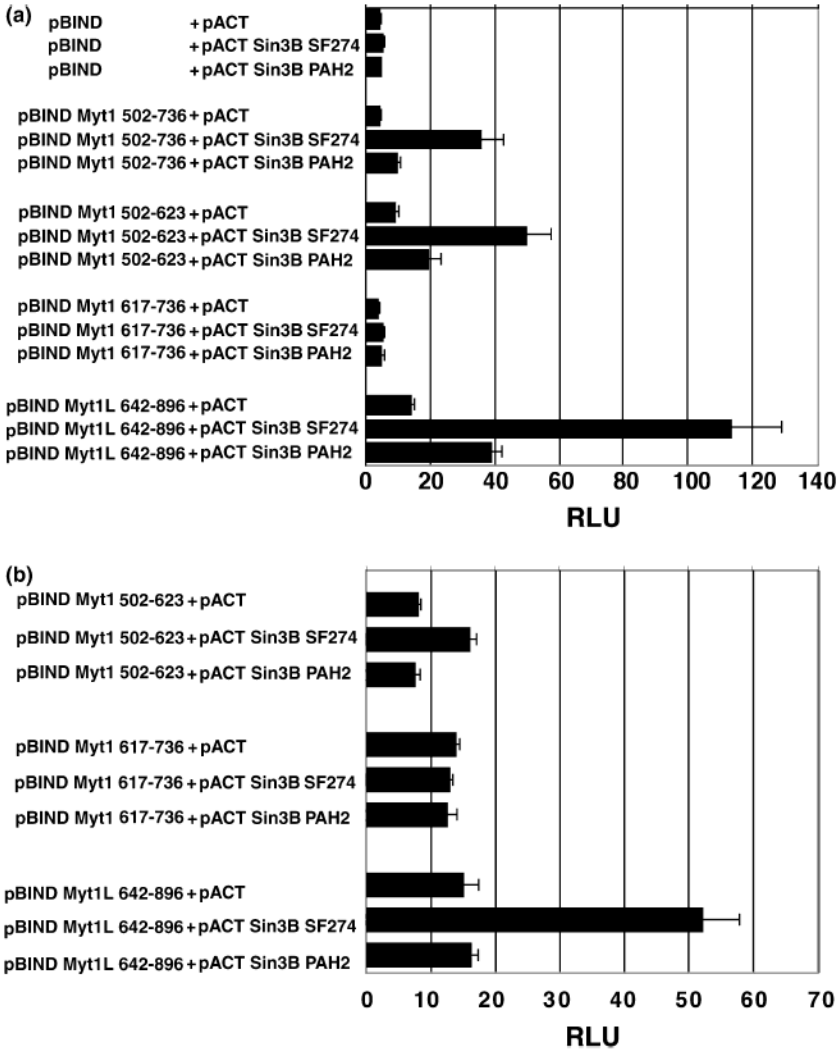

Fig. 3.

Myt1 and Myt1L interact with a single PAH domain in a mammalian two-hybrid assay in COS-1 and CG4 cells. (a) COS-1 cells and (b) CG4 cells were co-transfected with one PAH domain ($Sin3B_{PAH2}$) or two PAH domains ($Sin3B_{SF274}$) in the pACT vector together with either the central domain of Myt1 ($Myt1_{502–736}$), the amino terminal portion of the Myt1 central domain ($Myt1_{502–623}$), the carboxy terminal portion of the Myt1 central domain ($Myt1_{617–736}$) or the central domain of Myt1L ($Myt1L_{642–896}$) in the pBIND vector. Results are expressed as the ratio of firefly to renilla luciferase light units (RLU).Values are mean ± SD of six replicates.

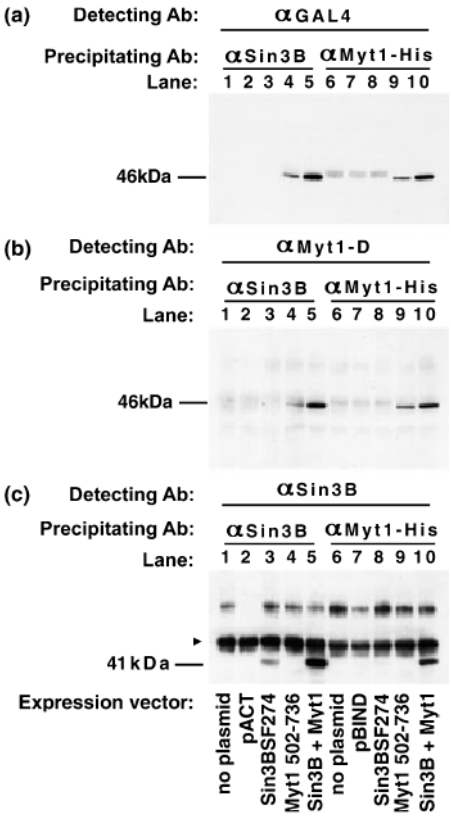

Fig. 4.

Co-immunoprecipitation of Myt1 and Sin3B. COS-1 cells were transfected with the indicated plasmids: no plasmid in lanes 1 and 6, the vector pACT control in lane 2, the pBIND control in lane 7, individual $Sin3B_{SF274}$ (lanes 3 and 8) or $Myt1_{502–736}$ (lanes 4 and 9) plasmids, or an equimolar mixture of $Sin3B_{SF274}$ and $Myt1_{502–736}$ plasmids (lanes 5 and 10). Complexes were precipitated with either an antibody directed against Sin3B (αSin3B; lanes 1–5) or Myt1 (αMyt1-His; lanes 6–10) and the individual components of these complexes were detected with antibodies against (a) GAL4 (αGAL4), (b) Myt1 (αMyt1-D) (c) Sin3B (αSin3B). The 46-kDa Myt1–GAL4 fusion protein (a and b) and the 41-kDa $Sin3B_{SF274}$–VP16 fusion protein (c) are indicated. The 55-kDa immunoglobulin heavy chain was also recognized by the Sin3B antibody (arrowhead in c). The gel images were taken from two independent immunoprecipitations.

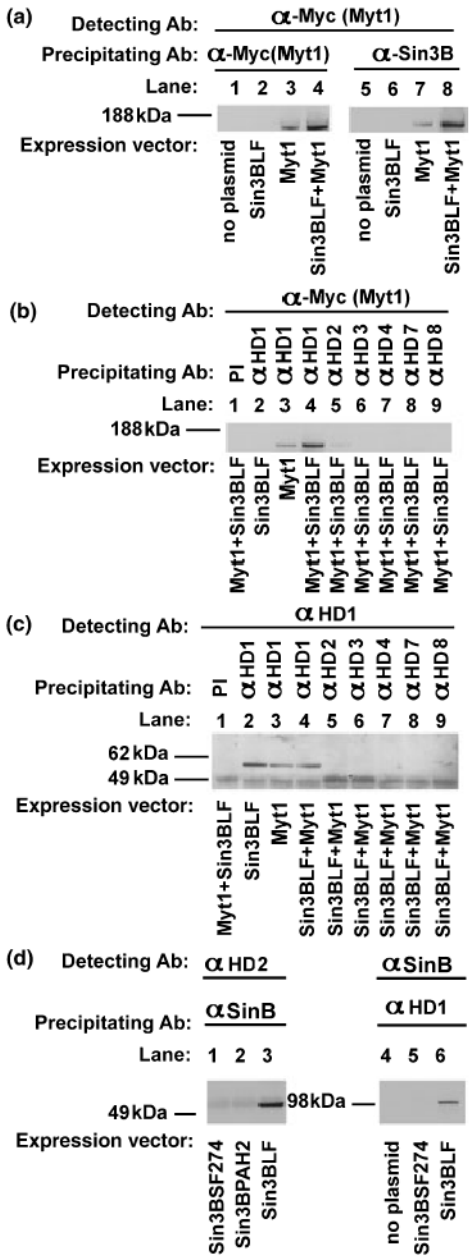

Fig. 5.

Co-immunoprecipitation of full-length Myt1 with HDACs. (a–c) HEK293 cells were transfected with plasmids encoding the Myc epitope-tagged full-length Myt1 (Myt1), $Sin3B_{LF}$ or equal amounts of both plasmids. (a) Proteins from transfected cells were immunoprecipitated with antibodies directed against the Myc epitope tag [α-Myc(Myt); lanes 1–4] or $Sin3B_{LF}$ (α-Sin3B; lanes 5–8), then detected with the anti-Myc antibody [α-Myc(Myt)]. (b and c) Proteins from transfected cells were immunoprecipitated with antibodies directed against HDAC1 (αHD1, lanes 2–4), HDAC2 (αHD2, lane 5), HDAC3 (αHD3, lane 6), HDAC4 (αHD4, lane 7), HDAC7 (αHD7, lane 8) and HDAC8 (αHD8, lane 9), and detected with antibodies directed against the Myc epitope tag (α-Myc(Myt); b) or HDAC1 (αHD1; c) or with preimmune serum (PI). Panel (c) shows that the HDAC1 antibody specifically detected HDAC1 (lanes 2–4) and did not cross-react with HDAC2 (lane 5). The gel images were taken

from three independent immunoprecipitations. (d) HEK293 cells were transfected with different Sin3B expression vectors, and immunoprecipitated with anti-sin3B antibody (αSinB) and detected with anti-HDAC2 antibody (αHD2) (lanes 1–3), or immunoprecipitated anti-HDAC1 antibody (αHD1) and detected with anti-Sin3B antibody (αSinB) (lanes 4–6).

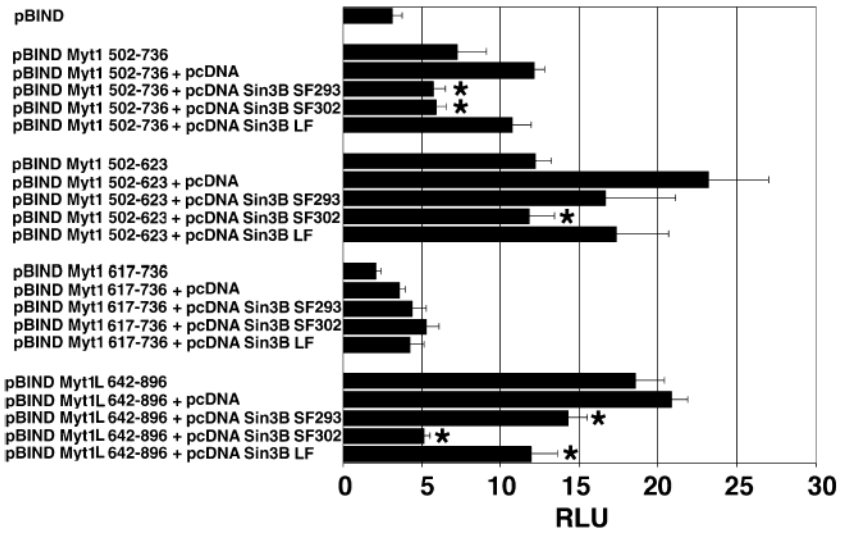

Fig. 6.

Myt1 and Myt1L repress the activity of a heterologous promoter. Plasmids encoding the Sin3B-interacting domain of Myt1 including $Myt1_{502–623}$, $Myt1_{502–736}$ or $Myt1L_{642–896}$ fused to the GAL4-binding domain in the pBIND vector were co-transfected with either $Sin3B_{LF}$, $Sin3B_{SF293}$ or $Sin3B_{SF302}$ together with the GAL4 promoter plasmid pG5 into COS-1 cells. Controls included the pBIND plasmid alone, each Myt1 or Myt1L plasmid co-transfected with the empty pcDNA3.1 plasmid, and the non-Sin3B-interacting domain of Myt1 (the carboxy terminal portion of the Myt1 central domain: $Myt1_{617–736}$). Results are expressed as the ratio of firefly to renilla luciferase light units (RLU). Values are mean ± SD of six replicates. *$p < 0.05$ versus mean of the two controls (different pBIND Myt1 vectors alone and pBIND Myt1 vectors plus empty pcDNA) (one-way anova).

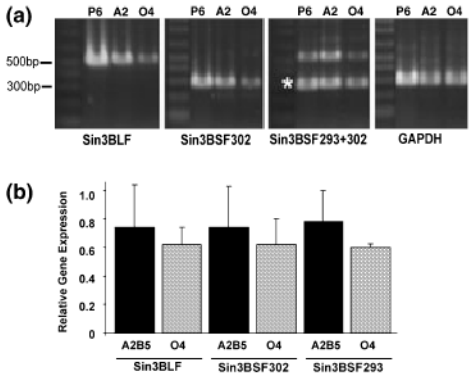

Fig. 7.

Oligodendrocytes express both the short and long forms of Sin3B. A2B5 + oligodendrocyte progenitors (A2) and O4 + oligo-dendrocytes (O4) were purified using flow cytometry and RNA was extracted for semiquantitative RT–PCR. (a) The linear range of the PCR reaction as determined by the first PCR cycle number detectable by gel electrophoresis is shown. The amplification primer pairs are listed below each gel. The asterisk denotes the $Sin3B_{SF293}$ band which was amplified when using the $Sin3B_{SF293+302}$ primers. Whole-brain lysate from postnatal day 6 (P6) mice was used as a positive control. (b) Gel bands were quantified using NIHimage software and the signal was normalized to GAPDH expression. Values are mean ± SEM for two independent experiments.